XXI ICTAM, 15–21 August 2004, Warsaw, Poland

A MICROMECHANICALLY BASED NETWORK MODEL FOR RUBBERY POLYMERS INCORPORATING MULLINS–TYPE STRESS SOFTENING

Serdar Göktepe, Christian Miehe
Institute of Applied Mechanics (Civil Engineering), Chair I, University of Stuttgart, Pfaffenwaldring 7
D-70550 Stuttgart, Germany

Summary We present a new micromechanically based constitutive model for the description of the Mullins–type stress softening observed in rubbery polymers. The constitutive approach, embedded in the full network theory, has a basic two–step procedure: (i) The set up micromechanically based constitutive models for a *single chain orientation* and (ii) the definition of the macroscopic stress response of the network by a directly evaluated micro–to–macro transition for a *discrete orientation space* over the *micro sphere*. Due to the inherent structure of the model, one dimensional scalar variables govern the model and the deformation–induced anisotropy is achieved.

Description of Mullins' Effect

Rubbery polymers exhibit deformation–induced stress softening behavior, so–called Mullins' effect, in particular under cyclic loadings. Mullins' effect is more pronounced in the filled stock than in the pure gum one. Due to the this fact, molecular scenarios based on the breakdown of the stiffening due to the fillers have been proposed since 1960s. In our work we follow the molecular damage theory originally proposed by Bueche [1] and further developed by Govindjee and Simo [2]. In this theory, the softening is based on the breaking of bonds between the chains and the fillers. In Figure 1a, a schematic picture of the filled polymer network, composed of three chains with different contour lengths $L_C > L_B > L_A$, is shown. In a extension of the network in horizontal direction, first the chain A will reach its limiting extensibility and detach from a particle. Due to the loss of contribution of the chain A to the network stiffness upon retraction of the network, its response will be softer. In a further extension of the filled network from the totally unloaded state, stress–stretch curve will trace the unloading path but beyond the previous maximum extension the longer chains reach their limiting extensions. Therefore, chain B and chain C might debond from the particles and further softening is observed in the unloading response. Softening in the stress-stretch behavior of the material in a typical quasi–static cyclic tensile uniaxial experiment is depicted schematically in Figure1b. The curves in the stress–stretch diagram are labeled as a, b, c, which correspond to the loading intervals with the same labels.

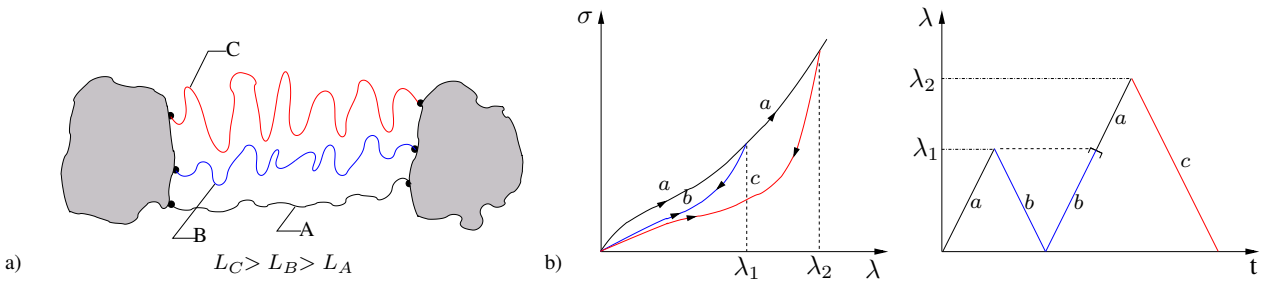

Figure 1. a) Schematic representation of the filled polymer network. Three chains, labeled as A, B and C, extending between two filler particles. Different contour lengths are assigned to each of them, $L_C > L_B > L_A$. b) Idealized description of Mullins' effect in a uniaxial cyclic tensile test. Stress–stretch response of the specimen is depicted along with corresponding loading function.

Constitutive Framework

During the addition of fillers in a sulfur vulcanization process of polymers, some of the chains constitute the network between fillers, so–called particle–to–particle (PP) network. Some of them, on the other hand, run between crosslinks so–called crosslink–to–crosslink (CC) network. Therefore, it is reasonable to decouple the total free energy into two parts, $\Psi = \Psi_{cc} + \Psi_{pp}$. Response of the CC network is described by the full network model recently proposed in Miehe et al. [4]. For the response of the PP network it is reasonable assume affine deformation due to the large size of the filler particles. Therefore, in the construction of constitutive model for PP network, we base the formulation on the affine version of the micro–sphere model. The free energy of the affine network Ψ_{af} is obtained by averaging of free energies of chains oriented in different directions over the unit sphere surface, see Figure2a,b.

$$\Psi_{af} = \langle n\psi(\bar{\lambda})\rangle := \frac{1}{|\mathcal{S}|}\int_{\mathcal{S}} n\psi(\bar{\lambda})dA \approx \sum_{i=1}^{np} n\psi_i(\bar{\lambda}_i)w_i \quad \text{where} \quad \bar{\lambda}_i = \sqrt{\boldsymbol{t}_i \cdot \boldsymbol{g}\boldsymbol{t}_i} \quad \text{and} \quad \boldsymbol{t}_i := \bar{\boldsymbol{F}}\boldsymbol{r}_i \tag{1}$$

In equation (1), continuous averaging integral over the continuous space directions is approximated by an effective discrete integration, see Figure2c. In (1), $\bar{\boldsymbol{F}}$ and $\boldsymbol{g}$ denote the isochoric part of the deformation gradient $\boldsymbol{F}$ and the current metric, respectively. Free energy in each direction has the celebrated Langevin form. Then Kirchhoff stresses read from Doyle–Ericksen formula $\bar{\boldsymbol{\tau}}_{af} = 2\partial_{\boldsymbol{g}}\Psi_{af} = \langle \beta\, \boldsymbol{t}\otimes\boldsymbol{t}\rangle = \sum_{i=1}^{np} w_i\beta_i\, \boldsymbol{t}_i\otimes\boldsymbol{t}_i$ with the micro stress components in each orientation $\beta_i := \mu(3N - \bar{\lambda}_i^2)/(N - \bar{\lambda}_i^2)$. In the stress expression, μ, N and w_i denote the shear modulus, the number of modules in a chain and the weighting factors, respectively. Following the observations reported in [2], Kirchhoff stresses contributed

by PP network, given in (2), is obtained by scaling the β_i with normalized stress function $\xi = \hat{\xi}(\bar{\psi}_i, d_i)$ where $\bar{\psi}_i$ and d_i stands for the normalized free energy computed in each direction i and the scalar damage parameter evolving in this orientation. The scaling function ξ has been found to be represented by family of curves each corresponding to the value of the damage d_i. Its explicit form is given by $\xi = \hat{\xi}(\bar{\psi}_i, d_i) = c_1(d_i)[\bar{\psi}_i - c_2(d_i)]^2 + c_3(d_i)$ with $c_m = k_m \exp((-1)^m \delta_m d_i)$ for $m \in \{1, 2, 3\}$. Here, k_m and δ_m are the additional material parameters.

$$\bar{\boldsymbol{\tau}}_{pp} = 2\partial_{\boldsymbol{g}} \Psi_{pp} = \langle \xi(\bar{\psi}, d)\beta \, \boldsymbol{t} \otimes \boldsymbol{t} \rangle = \sum_{i=1}^{np} w_i \xi(\bar{\psi}_i, d_i)\beta_i \, \boldsymbol{t_i} \otimes \boldsymbol{t_i} \, . \tag{2}$$

In order to complete the formulation, an evolution equation for the damage variable d_i is to be determined. The discontinuous evolution equation is canonically obtained in a thermodynamically consistent way by maximizing the dissipation in each direction with the constraint of a damage criterion function. The damage criterion function is assumed to have the form $\phi_i = \bar{\psi}_i - d_i \leq 0$, see Miehe and Göktepe [5] for the details of the algorithmic setting. It should be carefully noted that this type of damage formulations differ from the classical $(1 - d)$ theory in the sense that it is not possible to separate the damage parameters from the deformation. This feature of these models is essential for achieving correct shapes of hysteresis, see Göktepe [3] for the comparison of $(1 - d)$ theory with these type of models.

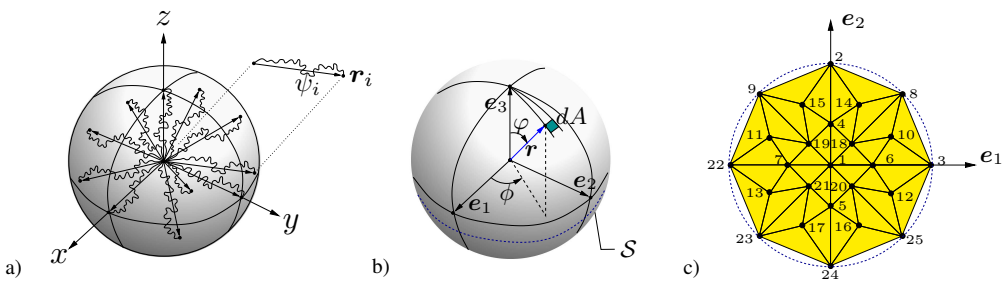

Figure 2. Unit sphere microstructure. a) Representation of network structure in the microsphere b) The orientation of unit vector $\boldsymbol{r}$ parameterized by spherical angles (ϕ, φ) c) Stereographic pole projection of the unit sphere. Numerical implementation uses $np = 21$ integration points for the discrete microstate evaluation on the sphere. The points 22–25 are introduced for plotting purposes.

Numerical Examples

The modeling capacity of the proposed constitutive approach is investigated with respect to the fitting of well known experimental data reported by Mullins and Tobin [6]. In Figure3a the performance of the proposed model is illustrated. It should be noted that set effect generally observed in the experiments at the zero stress level is obtained due to the inherent induced anisotropic feature of the model. In order to illustrate further the anisotropic feature of the model the simple shear test at a material point is performed. Deformation and corresponding deformation gradient is given in Figure3b. At the different stages of deformation, distribution of the softening is plotted on the pole figure, see also Figure2c. Evolution of the maximum damage orientation during the deformation is clearly depicted.

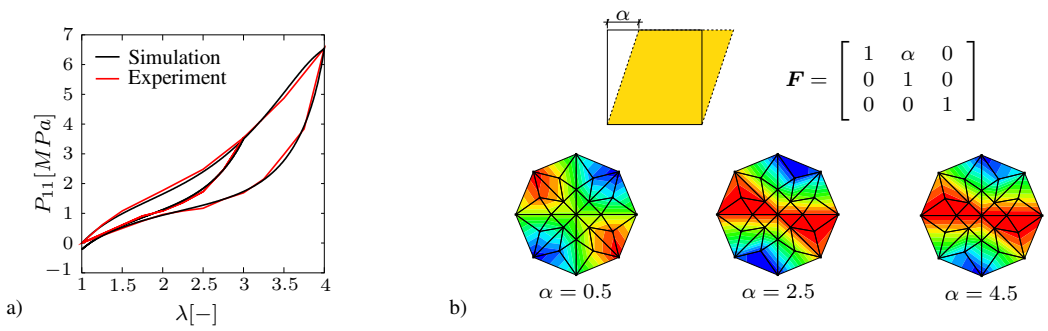

Figure 3. Numerical examples. a) Simulation of the test data reported by Mullins and Tobin [6] b) Distribution of damage over the microsphere in a simple shear test at different stages of loading. Damage is increasing from red zone to blue one.

References

[1] Bueche, F.: Molecular Basis for the Mullins Effect. *J. Appl. Poly. Sci*, **4**:107–114, 1960.

[2] Govindjee, S., Simo, J.: Transition from Micro-Mechanics to Computationally Efficient Phenomenology: Carbon Black-Filled Rubbers Incorporating Mullins' Effect. *J. Mech. Phys. Solids*, **40**:213–233, 1992.

[3] Göktepe, S.: A Micromechanically Based Constitutive Description of Elasticity and Damage in Rubberlike Materials. *MSc Thesis*, Report No. 02-I-02 of Institute of Applied Mechanics (Civil Engineering) Chair I, University of Stuttgart, 2002.

[4] Miehe, C., Göktepe, S., Lulei, F.: A Micro–Macro Approach to Rubber–Like Materials. Part I: The Non–Affine Micro–Sphere Model of Rubber Elasticity. *J. Mech. Phys. Solids*, in press, 2003.

[5] Miehe, C., Göktepe, S.: A Micro–Macro Approach to Rubber–Like Materials. Part III: The Micro–Sphere Model incorporating Mullins' Effect. To appear in *J. Mech. Phys. Solids*, 2004.

[6] Mullins, L., Tobin, N.R.: Theoretical Model for the Elastic Behavior of Filler Reinforced Vulcanized Rubbers. *Rubb. Chem. Technol.*, **30**:555–571, 1957.